Materials Transactions, Vol. 61, No. 5 (2020) pp. 856 to 861
Special Issue on Materials Science on Mille-Feuille Structure

Introduction of Mille-Feuille-Like α/β Layered Structure into Ti–Mo Alloy

Satoshi Emura* and Xin Ji

Research Center for Structural Materials, National Institute for Materials Science, Tsukuba 305-0047, Japan

As a trial to realize kink band strengthening in titanium alloys, slight cold rolling followed by aging heat treatment were applied on Ti–12 mass% Mo alloys for obtaining mille-feuille-like layered hcp (α)/bcc (β) two phase structure. After slight cold rolling at rolling reduction of 5% and subsequent aging heat treatment at 973 K for 180 ks, plate-like α phases were precipitated in the β phase matrix and made an alternately stacked mille-feuille-like α/β layered structure. These α phases were precipitated on the boundary of $\{3\ 3\ 2\}\langle 1\ 1\ 3\rangle$ β type deformed twins introduced in the β phase matrix during the slight cold rolling. The thin film-like α phase precipitated at a very early stage of aging, and became thicker during aging to produce the mille-feuille-like α/β layered structure. [doi:10.2320/matertrans.MT-MM2019002]

(Received August 29, 2019; Accepted February 10, 2020; Published March 13, 2020)

Keywords: *titanium molybdenum alloys, slight cold rolling, aging heat treatment, mille-feuille-like α/β layered structure, $\{3\ 3\ 2\}\langle 1\ 1\ 3\rangle$ β twinning*

1. Introduction

In 2001, a high strength Mg–Zn–Y alloy with superior tensile yield strength of 610 MPa and reasonable elongation of 5% was developed.[1] The microstructure was composed of fine hcp-Mg grains and fine lamellar grains with a novel long-period stacking ordered (LPSO) structure, which has a long-period chemical ordered structure along with an LPSO structure.[2] This LPSO structure was also found in the Mg–Zn–Gd alloy[3] and other Mg–Zn–rare earth (RE) alloys,[4] which also showed both high strength and good ductility.

Yoshimoto *et al.* investigated the cast and extruded Mg–Zn–Y alloys with a good balance of tensile strength and elongation, and reported that not only the microstructural refinement and dispersion of the lamellar phase with high deformation resistance but also the bent LPSO structure with random grain boundaries were found after extrusion, which seemed to be one of the causes of the high strength and ductility.[5] Hagihara *et al.* investigated the deformation behavior of the $Mg_{12}YZn$ LPSO phase produced by directional solidification.[6] In addition to the dominant $(0\ 0\ 0\ 1)\langle 1\ 1\ \bar{2}\ 0\rangle$ basal slip, they reported the formation of the kink band structures, which contributed to the deformation during the compression test. They extensively investigated the role of the deformation kink on the mechanical properties of various directionally solidified and extruded Mg alloys with LPSO structure and concluded that both the formation stress of the kink band and the hindering effect of the kink bands on the motion of basal dislocation contributed to the strengthening of LPSO alloys.[7]

It should be noted that the kink deformation is not a peculiar deformation mode in Mg alloys, which has also been reported in other metals such as Cd[8] and Zn,[9] especially in those with strong plastic anisotropy.[7] Inamura recently analyzed the geometrics of kink bands and suggested that there exists a compatible kink microstructure to annihilate the disclinations inevitably introduced through kink band formation and that this stable kink microstructure contributes to the strengthening of materials.[10] This theory is purely geometric and is applicable to other alloys and materials.

*Corresponding author, E-mail: EMURA.Satoshi@nims.go.jp

In Ti alloys, the kink deformation has been observed in the lamellar type hcp (α)/bcc (β) two phase structure.[11,12] Furthermore, the kink band has been observed in stable β single phase alloys.[13,14] Strengthening by kink band formation (kink band strengthening) has not been confirmed in Ti alloys. However, it would be very useful if kink band strengthening could be successfully introduced into Ti alloys. The α phase is a dominant phase in Ti alloys, and it has the same hcp structure as Mg. However, its main deformation mode is a prismatic slip, not a basal slip such as that in Mg.[15–17] Therefore, the investigation of the possibility of kink band formation and kink band strengthening in Ti alloys seems to be also meaningful to understand the details of kink bands in Mg alloys through the comparison of these two alloys.

To realize the kink band formation in Ti alloys during deformation such as compression test, an α/β layered structure similar to the lamellar structure (hereafter we call the layered structure as mille-feuille-like structure) seems to be favorable due to their plastic anisotropy. Furthermore, the α phase, with fewer slip systems than the β phase, should be mainly deformed. For that purpose, we selected the Ti–Mo binary alloy system for the investigation, because the precipitated α phase in this alloy system is softer than the matrix β phase owing to the lack of the α phase strengthening element of Al.[18] Further, to make the mille-feuille-like α/β layered structure in Ti–Mo alloys, we followed the process that Miura *et al.* applied on Al–Ag alloys, namely, slight cold rolling followed by aging heat treatment.[19]

In this study, as a trial to realize kink band strengthening in Ti alloys, slight cold rolling and subsequent aging heat treatment were applied on Ti–Mo alloys to introduce a mille-feuille-like α/β layered structure. The α phase precipitation behavior during the aging heat treatment was also reported.

2. Experimental Procedure

A Ti–12Mo alloy (mass%, same as below) ingot, approximately 70 mm in diameter and 1.2 kg in weight, was prepared by cold crucible levitation melting. The ingot was hot forged to a 40-mm-square slab at 1273 K and hot rolled into a plate with 5-mm-thickness at 1073 K. After removing

the surface oxidation layer to 3-mm-thickness, the plate was cold rolled into a plate with 1-mm-thickness. The rolled plate was solution treated (ST) at 1173 K for 18 ks to obtain a β single phase sample with coarse equiaxed grains. To obtain a large layered α precipitation, coarse equiaxed β grains are preferable. The heat treated plate with 50-mm-width was cut into small pieces with 50-mm-length and 5-mm-width. Some pieces were slightly cold rolled with the reduction rate of 5%. The slight cold rolling direction was orthogonal to the hot rolling and initial cold rolling direction. We will refer to these samples with slight cold rolling as CR samples. We also examined the samples without slight cold rolling (just after solution treatment) as ST samples. Both CR and ST samples were aged at 973 K for 180 ks for precipitation of the α phase, followed by water quenching. The principal axes of the rolled samples are defined as follows.[18] The axis corresponding to the rolling direction is referred to as RD; the one normal to the rolling plane is ND; and the one normal to RD and ND is TD. The RD plane is the plane normal to the RD; and the TD plane is the plane normal to the TD. To check the microstructure evolution, the CR samples were also heat treated at 973 k for 60 s, 7.2 ks, and 36 ks, respectively. Microstructural observations were performed using optical microscopy (OM), scanning electron microscopy (SEM), electron backscattered diffraction (EBSD) and transmission electron microscopy (TEM). The TEM samples was cut from specified positions and lifted out by a manipulator by using a dual-beam focused ion beam.

3. Results and Discussion

Figure 1 shows the SEM back scattered electron (BSE) image of an ST sample taken from the TD plane. In all the OM, SEM, and EBSD figures in this work, the vertical direction is ND. Coarse equiaxed β grains with the grain size of some hundred micrometers were obtained after ST. Figure 2 exhibits the OM images of a CR sample after aging at 973 K for 180 ks. Figure 2(a) was taken from the TD plane, and Fig. 2(b) was taken from the RD plane. Many plate-like precipitates were observed inside of the β grains. Some grains had a mille-feuille-like layered structure of precipitates, and others had an intersected structure of precipitates. As both the TD and RD planes have layered structure of precipitates, these precipitates are considered to be three-dimensionally stacked. Figure 3 shows the SEM BSE magnified view of a layered structure of precipitates taken from the TD plane. Alternately stacked bright and dark phases were observed. The dark phases had very thin thickness, of mostly less than 1 μm. The bright phases were thicker than the dark phases, and some bright phases include small dark precipitates. Figure 4(a) shows the SEM BSE image of a CR sample after aging at 973 K for 180 ks taken from the TD plane, and Fig. 4(b)–(f) show the EBSD analysis results from the same areas as those in Fig. 4(a). EBSD phase map (Fig. 4(b)) indicates that the dark and bright phases in SEM BSE images (Fig. 3 and Fig. 4(a)) correspond to α and β phases, respectively. In BSE images, phases with larger amount of heavy elements (elements with large atomic number) exhibit brighter contrast. The amount of Mo in β phase is larger than that in α phase, so α and β phases exhibit dark and bright contrast, respectively. Thus, the layered structure observed in the CR sample after aging was confirmed as an α/β layered

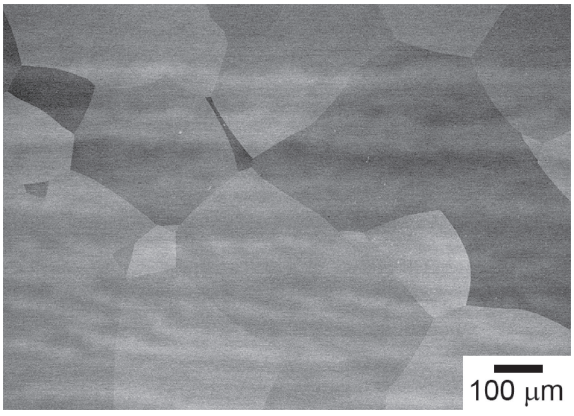

Fig. 1 SEM BSE image of ST sample taken from the TD plane.

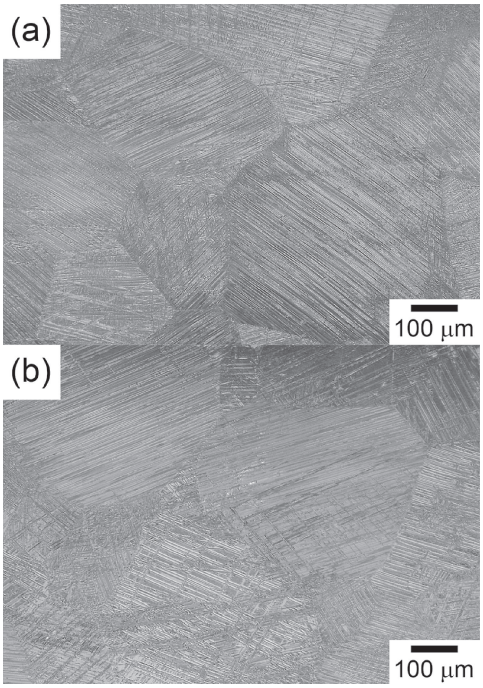

Fig. 2 OM images of CR sample after aging at 973 K for 180 ks; (a) taken from the TD plane, and (b) taken from the RD plane.

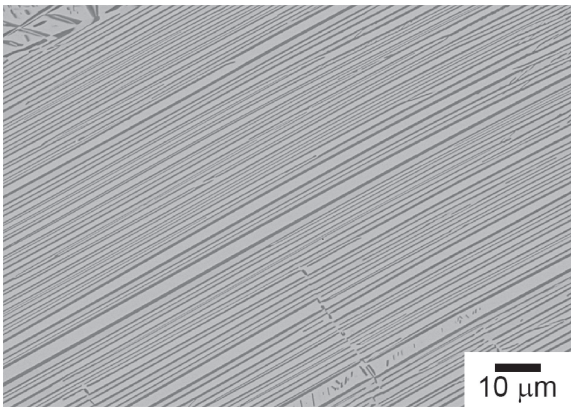

Fig. 3 SEM BSE magnified view of layered structure of precipitates taken from the TD plane.

structure. Figure 4(c), (d), (e), and (f) show the EBSD inverse pole figure (IPF) maps of the α phase for the TD direction (Fig. 4(c)) and for the RD direction (Fig. 4(d)), and IPF maps of the β phase for the TD direction (Fig. 4(e)) and for the RD direction (Fig. 4(f)), respectively. In the α/β layered structure, α phases have the same direction in one β grain, but β phases have two different directions alternately. Figure 5 shows the TEM images of the α/β layered structure in a CR sample after aging at 973 K for 180 ks. From the selected area electron diffraction (SAED), the orientation relationship of (0 0 0 2) α//(1 1 0) β was confirmed, which follows the Burgers orientation relationship.[20,21] It is worth noting that weak spots from ω phase with two variants can also be observed in the SAED image. Since the present study is focusing on the formation of α/β layered structure, the ω phase is not discussed here. Figure 6 shows the SEM BSE image of an ST sample (without 5% cold rolling) after aging at 973 K for 180 ks taken from the TD plane. Dark phases (α phases) were mainly precipitated with acicular structure inside the β grain and were also precipitated with film-like structure on the primary β grain boundary. No layered structure was found without slight cold rolling, so the slight cold rolling is necessary for introducing a mille-feuille-like α/β layered structure into the Ti–12Mo alloy.

To investigate the α phase precipitation behavior in the CR sample, first we observed the microstructure of this sample before aging (As CR sample). Figure 7 shows OM images of the As CR sample taken from the TD plane. Plate-like features, which had similar morphology as the precipitated α phases after aging, can be observed in Fig. 7. Figure 8 exhibits the EBSD analysis results from the TD plane of the As CR sample. Figure 8(a) shows the IPF map of the β phase

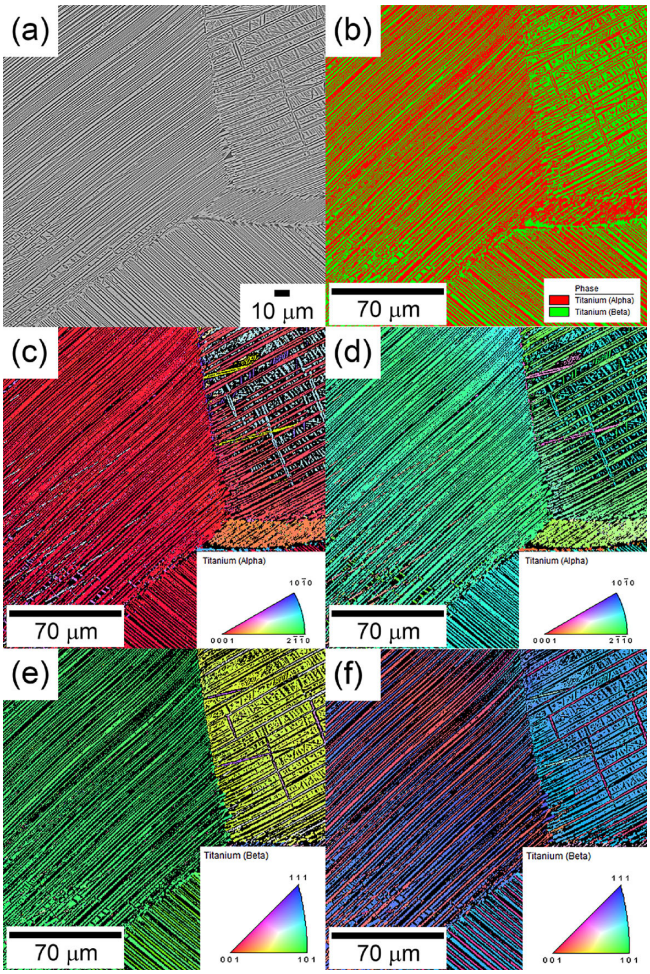

Fig. 4 (a) SEM BSE image of CR sample after aging at 973 K for 180 ks taken from the TD plane, (b) EBSD phase map, (c) EBSD IPF map of α phase for the TD direction, (d) EBSD IPF map of α phase for the RD direction, (e) EBSD IPF map of β phase for the TD direction, and (f) EBSD IPF map of β phase for the RD direction.

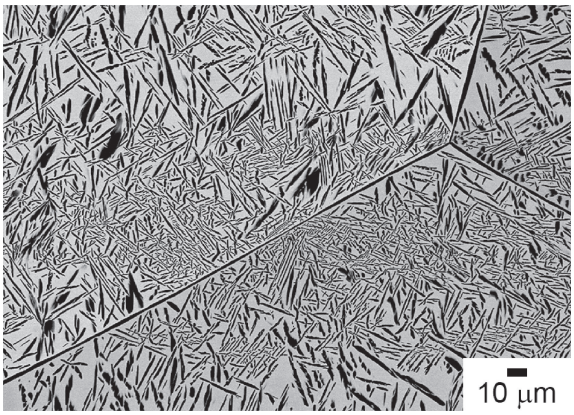

Fig. 6 SEM BSE image of ST sample (without 5% cold rolling) after aging at 973 K for 180 ks taken from the TD plane.

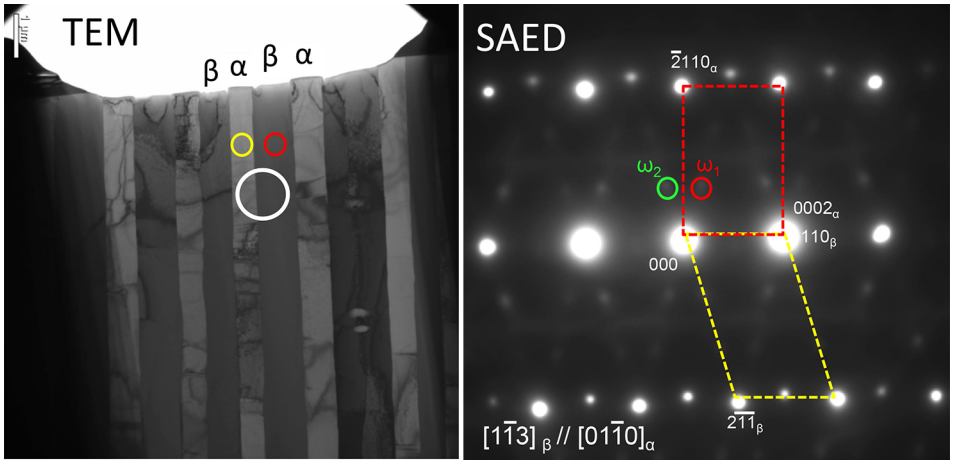

Fig. 5 TEM images of α/β layered structure in CR sample after aging at 973 K for 180 ks.

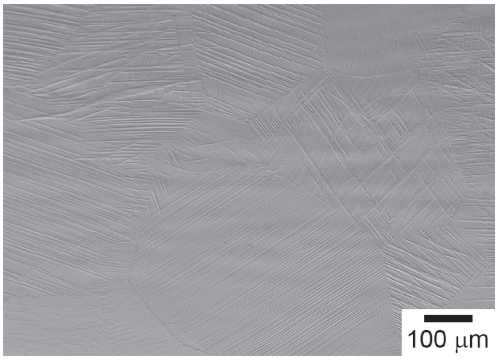

Fig. 7 OM image of As CR sample taken from TD plane.

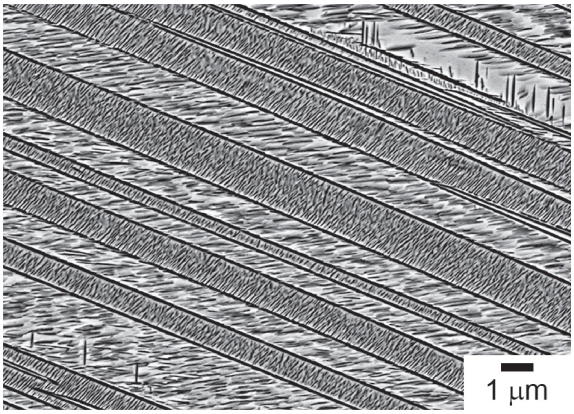

Fig. 9 SEM BSE image of CR sample after aging at 973 K for 60 s taken from the TD plane.

for the TD direction, and Fig. 8(b) indicates the boundaries with a misorientation angle of 50.5° along the ⟨1 1 0⟩ direction as red lines, which correspond to the {3 3 2}⟨1 1 3⟩ β twin boundaries.[22,23] From the EBSD analysis shown in Fig. 8, the plate-like features observed in the As CR sample are identified as {3 3 2}⟨1 1 3⟩ β twins. The {3 3 2}⟨1 1 3⟩ β twinning, which is an unusual twinning mode in bcc metals because neither the twinning plane nor the twinning direction is close-packed, was first experimentally found in Ti–11.5Mo–6Zr–4.5Sn alloy.[24] This {3 3 2}⟨1 1 3⟩ β twinning system is so far found only in metastable β titanium alloys, including Ti–Mo alloys, and is considered to be the main reason of the high work hardening rate and the resultant large elongation during tensile deformation in metastable β titanium alloys.[25–27]

Next, we observed the CR sample after aging at 973 K for 60 s to check the very early stage of α phase precipitation. To be accurate, the sample was put into the furnace with the temperature of 973 K, kept for 120 s to recover the furnace temperature, aged for 60 s at 973 K, and then water quenched. Figure 9 shows the SEM BSE image of the CR sample after aging at 973 K for 60 s taken from the TD plane. Film-like thin α phases with width of approximately 100 nm were precipitated on the twin boundaries. Furuhara reported that a similar film-like α phase forms on the (3 3 $\bar{2}$)[1 1 3] β twin boundary in Ti–15V–3Cr–3Sn–3Al after rolling at 77 K followed by aging at 933 K for 1.8 ks.[28] Ohyama also found the α phase nucleation and coalescence on the twin boundary in Ti–16V–10Sn alloy after 5% cold rolling followed by aging at 873 K for 259.2 ks, although its morphology was far from a straight line, such as that observed in Fig. 9.[29] It is suggested that the formation of {3 3 2}⟨1 1 3⟩ β twin boundaries by slight cold rolling offer effective sites for α phase nucleation, which is the key for making the mille-feuille-like α/β layered structure. Other than the film-like twin boundary α phase, finer α precipitates were found in the β matrix. As can be seen in Fig. 9, the high and low density α precipitate regions exist alternately. Hanada observed a high density of dislocations in the twinned area in a slightly (less than 2%) deformed Ti–22V alloy.[25] These high-density dislocations seem to be another preferential nucleation site for the α phase. In addition, the sample was 5% cold rolled before aging. Thus, even the untwinned area should have some defects due to cold rolling, which behave as α phase nucleation sites. Figure 10 shows the TEM images of α precipitates in a CR sample after aging at 973 K for 60 s. As in the sample after aging for 180 ks, the twin boundary α phase and β matrix phase had an orientation relationship of (0 0 0 2) α//(1 1 0) β. This relationship has also been confirmed by EBSD pole figure analysis. Some α phases inside the β matrix phase had the same variant as the twin boundary α phase, but others did not. The twin boundary α phase and β matrix phase also had an orientation relationship

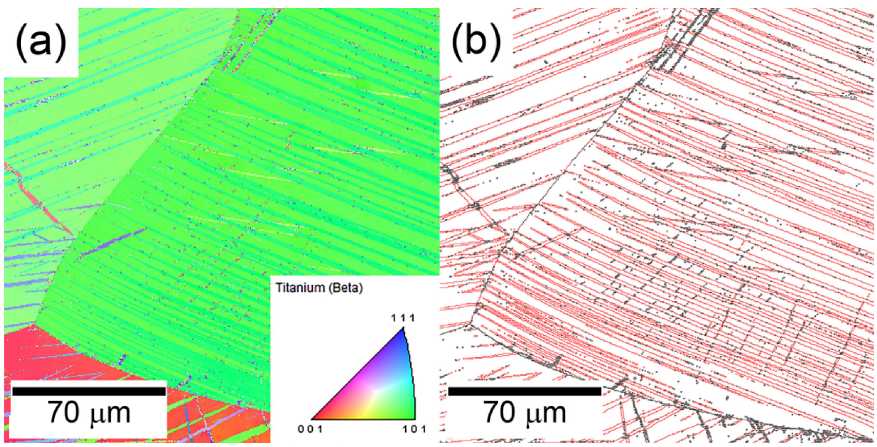

Fig. 8 EBSD analysis results from TD plane of As CR sample; (a) IPF map of β phase for the TD direction, and (b) boundaries with a misorientation angle of 50.5° along the ⟨1 1 0⟩ direction shown as red lines, which correspond to the {3 3 2}⟨1 1 3⟩ twin boundaries.

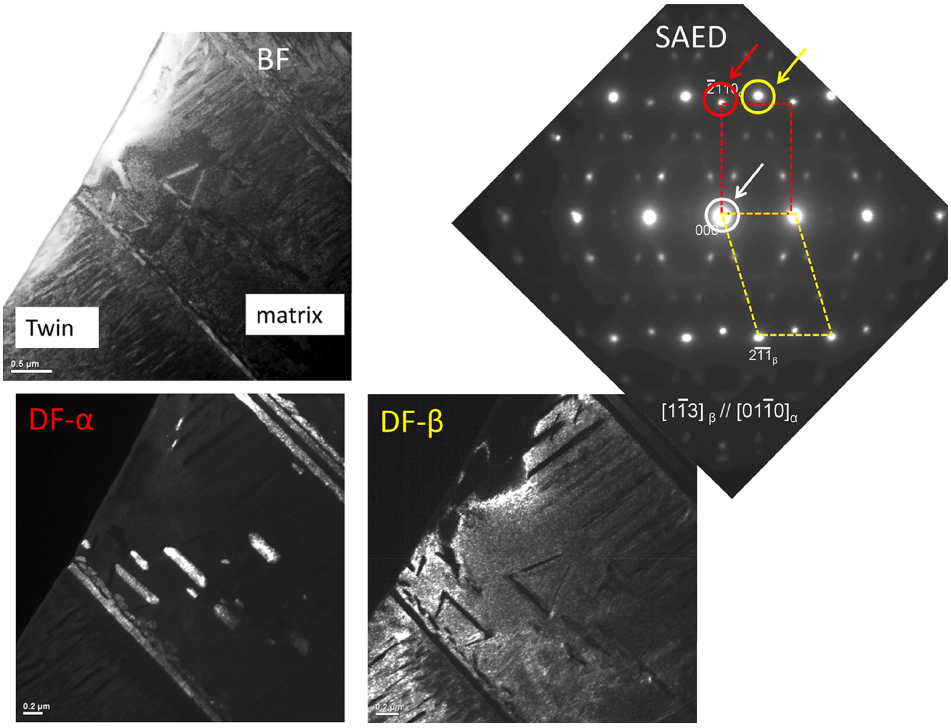

Fig. 10 TEM images of α precipitates in CR sample after aging at 973 K for 60 s.

of [0 1 $\bar{1}$ 0] α//[1 1 3] β. Similar relationship was confirmed by Furuhara,[28] and thus, the twin boundary α phase was considered to be precipitated in similar manner as Furuhara observed.

As shown in Fig. 9, at the very early stage of aging (60 s) at 973 K, not only twin boundary α phases but also finer α precipitates inside the β matrix were found. However, after long time aging (180 ks), only twin boundary α phases existed (and thickened) and the α precipitates inside the β matrix almost disappeared, as can be seen in Fig. 3. To investigate this microstructure evolution behavior, the CR samples with intermediate aging periods were observed. Figure 11(a) and (b) exhibit the SEM BSE images of a CR sample taken from the TD plane after aging at 973 K for 7.2 ks and 36 ks, respectively. As the aging period became longer, the twin boundary α phases became thicker and the α precipitates inside the β matrix became smaller. Therefore, during aging at 973 K, the initial complicated α precipitates changed to a mille-feuille-like α/β layered structure through an Ostwald-like ripening process.[30]

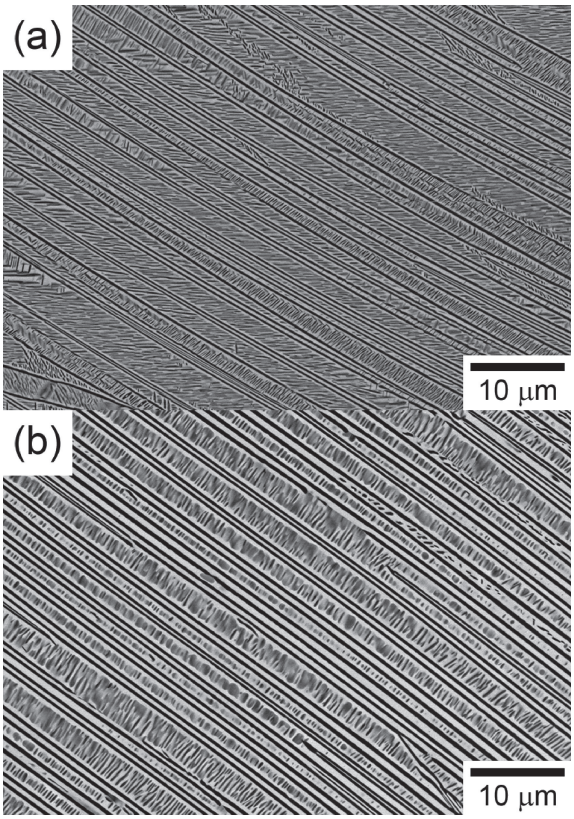

Fig. 11 SEM BSE images of CR sample taken from the TD plane after aging at 973 K for (a) 7.2 ks and (b) 36 ks.

4. Conclusion

The microstructure evolution of mille-feuille-like layered α/β structure by slight cold rolling and subsequent aging heat treatment has been investigated in Ti–12 mass% Mo alloy. After 5% slight cold rolling and the following aging heat treatment at 973 K for 180 ks, many plate-like α precipitates were observed inside of equiaxed β grains. An alternately stacked mille-feuille-like α/β layered structure was found in both the TD and RD planes. Just after slight cold rolling, many plate-like features were observed and confirmed as {3 3 2}⟨1 1 3⟩ β twins, which are the typical twinning system in metastable β titanium alloys. After a short-period aging of 60 s, very thin film-like α phases were precipitated on the twin boundaries, along with fine α precipitates inside the β matrix. The film-like twin boundary α phase became thicker and the fine α precipitates inside the β matrix became

smaller during aging, and finally the mille-feuille-like α/β layered structure was completed.

Acknowledgements

This study was supported by JSPS KAKENHI for Scientific Research on Innovative Areas "MFS Materials Science (Grant Number JP18H05482)". The authors thank Mr. S. Iwasaki, Mr. K. Iida, Mr. M. Kobayashi, and Mr. T. Hibaru for melting and plastic working of Ti–12Mo samples.

REFERENCES

1) Y. Kawamura, K. Hayashi, A. Inoue and T. Masumoto: Mater. Trans. **42** (2001) 1172–1176.
2) E. Abe, Y. Kawamura, K. Hayashi and A. Inoue: Acta Mater. **50** (2002) 3845–3857.
3) M. Yamasaki, T. Anan, S. Yoshimoto and Y. Kawamura: Scr. Mater. **53** (2005) 799–803.
4) Y. Kawamura and M. Yamasaki: Mater. Trans. **48** (2007) 2986–2992.
5) S. Yoshimoto, M. Yamasaki and Y. Kawamura: Mater. Trans. **47** (2006) 959–965.
6) K. Hagihara, N. Yokotani and Y. Umakoshi: Intermetallics **18** (2010) 267–276.
7) K. Hagihara, M. Yamasaki, Y. Kawamura and T. Nakano: Mater. Sci. Eng. A **763** (2019) 138163.
8) E. Orowan: Nature **149** (1942) 643–644.
9) J.B. Hess and C.S. Barrett: Metall. Trans. **185** (1949) 599–606.
10) T. Inamura: Acta Mater. **173** (2019) 270–280.
11) S.L. Semiatin, V. Seetharaman and I. Weiss: Mater. Sci. Eng. A **263** (1999) 257–271.
12) B. Perumal, M.A. Rist, S. Gungor, J.W. Brooks and M.E. Fitzpatrick: Metall. Mater. Trans. A **47** (2016) 4128–4136.
13) Y. Zheng, W. Zeng, Y. Wang, D. Zhou and X. Gao: J. Alloy. Compd. **708** (2017) 84–92.
14) Y. Zheng, W. Zeng, Y. Wang and S. Zhang: Mater. Sci. Eng. A **702** (2017) 218–224.
15) I.P. Jones and W.B. Hutchinson: Acta Metall. **29** (1981) 951–968.
16) F. Bridier, P. Villechaise and J. Mendez: Acta Mater. **53** (2005) 555–567.
17) L. Wang, Z. Zheng, H. Phukan, P. Kenesei, J.S. Park, J. Lind, R.M. Suter and T.R. Bieler: Acta Mater. **132** (2017) 598–610.
18) X.H. Min, L. Zhang, K. Sekido, T. Ohmura, S. Emura, K. Tsuchiya and K. Tsuzaki: Mater. Sci. Technol. **28** (2012) 342–347.
19) S. Miura, K. Ikeda and S. Emura: Collected Abstracts of 2018 Spring Meeting of The Japan Institute of Metals and Materials, (2018) S7.10 (DVD).
20) W.G. Burgers: Physica **1** (1934) 561–586.
21) D. Bhattacharyya, G.B. Viswanathan, R. Denkenberger, D. Furrer and H.L. Fraser: Acta Mater. **51** (2003) 4679–4691.
22) X.H. Min, K. Tsuzaki, S. Emura and K. Tsuchiya: Mater. Sci. Eng. A **528** (2011) 4569–4578.
23) T. Furuta, S. Kuramoto, J.H. Hwang, K. Nishino and T. Saito: Mater. Trans. **46** (2005) 3001–3007.
24) M.J. Blackburn and J.A. Feeney: J. Inst. Met. **99** (1971) 132–134.
25) S. Hanada and O. Izumi: Metall. Trans. A **17** (1986) 1409–1420.
26) S. Hanada and O. Izumi: Metall. Trans. A **18** (1987) 265–271.
27) S. Hanada, T. Yoshio and O. Izumi: Trans. JIM **27** (1986) 496–503.
28) T. Furuhara, H. Nakamori and T. Maki: Mater. Trans. JIM **33** (1992) 585–595.
29) H. Ohyama, H. Nakamori, Y. Ashida and T. Maki: ISIJ Int. **32** (1992) 222–231.
30) P.W. Voorhees, G.B. Mcfadden and R.F. Boisvert: Acta Metall. **36** (1988) 207–222.